



The MAGIC telescope for gamma-ray astronomy above 30 GeV

A. Moralejo for the MAGIC collaboration

Dipartimento di Fisica, Università di Padova and INFN Sezione di Padova, via Marzolo 8, 35131 Padova, Italy - e-mail: moralejo@pd.infn.it

Abstract. The MAGIC telescope is presently at its commissioning phase at the Roque de los Muchachos Observatory (ORM) on the island of La Palma. MAGIC will become the largest ground-based gamma ray telescope in the world, being sensitive to photons of energies as low as 30 GeV. The spectral range between 10 and 300 GeV remains to date mostly unexplored. Observations in this region of the spectrum are expected to provide key data for the understanding of a wide variety of astrophysical phenomena belonging to the so-called “non thermal Universe”, like the processes in the nuclei of active galaxies, the radiation mechanisms of pulsars and supernova remnants, and the enigmatic gamma-ray bursts. An overview of the telescope and its Physics goals is presented.

Key words. Gamma ray astronomy – Cherenkov telescopes

1. Introduction

Gamma ray astronomy has undergone in the last few years a spectacular development, led by the success of the CGRO (Compton Gamma Ray Observatory) mission, whose instruments have revealed a very high energy Universe far more rich than expected. The EGRET telescope aboard CGRO performed an all-sky gamma-ray survey above 100 MeV and produced a catalog of 271 sources (Hartman et al. 1999), of which 66 have been confirmed to belong to the blazar subclass of AGNs, six are galactic pulsars and the vast majority are to date unidentified. CGRO was operational between 1991 and 2000. The same years saw the advent of ground-based gamma ray astronomy, starting in 1989 with the first statistically sig-

nificant detection of a source, the Crab Nebula, by the Whipple Cherenkov telescope (Weekes et al. 1989). Following the Crab, the extragalactic objects Mkn-421 and Mkn-501 were detected. The latter had not been seen before by any space-based gamma-ray instrument, therefore proving the usefulness of the technique of the Whipple telescope: the observation of atmospheric Cherenkov light emitted by the particle showers initiated by gamma radiation on entering the atmosphere. Other instruments based on the same principle (HEGRA, CANGAROO, CAT) have confirmed the results of Whipple and in all detected more than 10 gamma ray sources at energies around 1 TeV.

2. The IACT technique

The thickness of the atmosphere of the Earth (about 28 radiation lengths at sea level) pre-

Send offprint requests to: A. Moralejo

Correspondence to: Dipartimento di Fisica, Università di Padova, via Marzolo, 8 35131 Padova

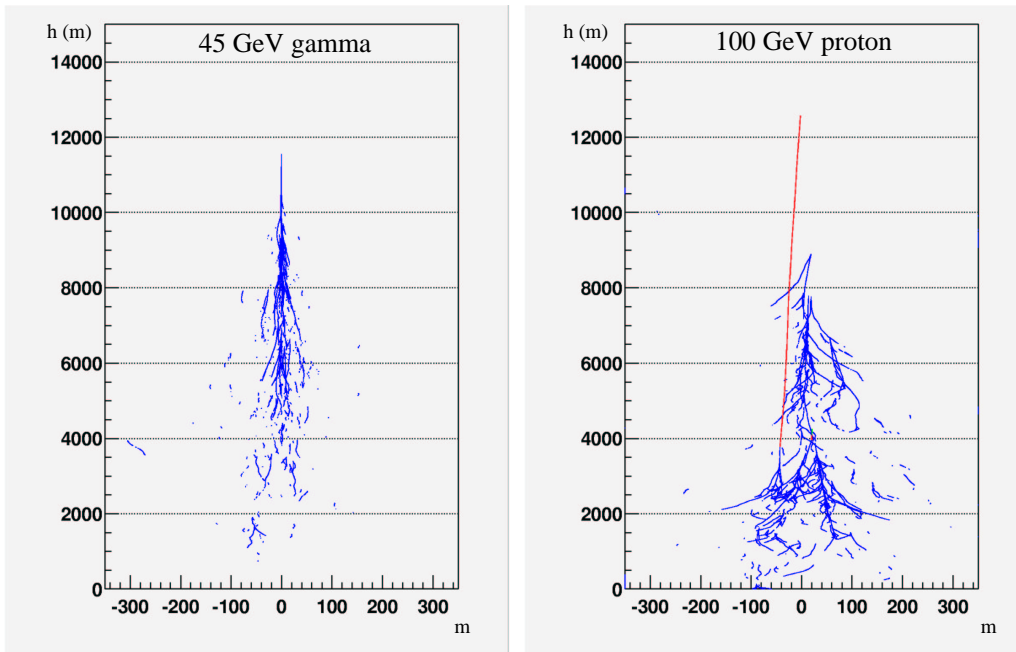


Fig. 1. Longitudinal development of a gamma- and a proton-initiated air shower. The vertical axis represents the height above the observation level, fixed at 2200 m a.s.l. Only the trajectories of Cherenkov emitting particles are shown. Almost all of the tracks in the plots correspond to electrons and positrons. An exception is the long track on the proton shower, between 13 and 3 km height, which belongs to a muon. The energies have been chosen such that the amount of produced Cherenkov light is comparable in both cases.

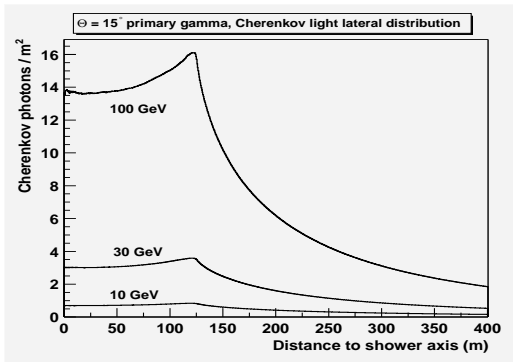


Fig. 2. Average Cherenkov light density at 2200 m above sea level, as a function of the distance to the shower axis, for showers initiated by gamma rays of 10, 30 and 100 GeV.

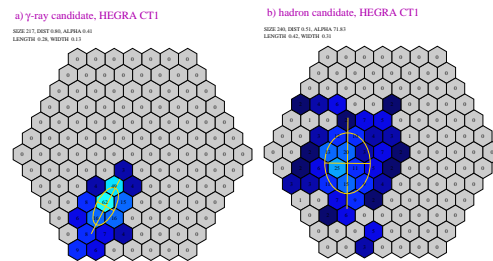


Fig. 3. Typical images of a gamma ray (left) and a hadron-initiated shower (right), obtained with the HEGRA CT1 telescope. Note that the major axis of the gamma image is oriented towards the camera center, where the source is located.

vents direct detection of high energy photons by ground-based instruments, even from the

top of the highest mountains. However, the effects of the absorption of a gamma ray of a few giga electron Volt (GeV) or more in the atmo-

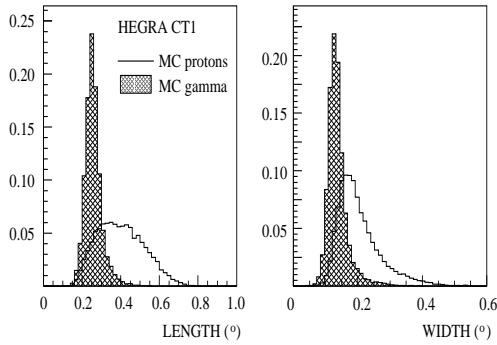


Fig. 4. Image analysis on data from the HEGRA CT1 telescope (Kranich 2002). The RMS of the light distribution along the major and the minor axis of the image are called respectively LENGTH and WIDTH, and along with other image parameters are a key tool to discriminate the gamma events from the background of cosmic ray showers.

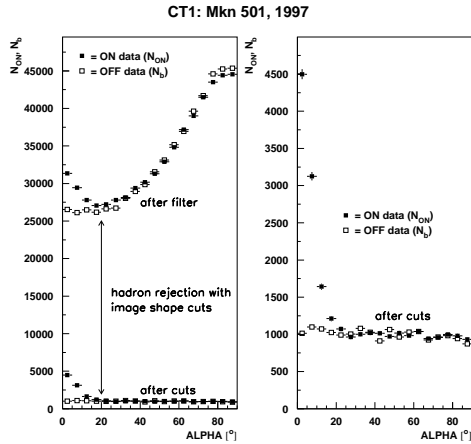


Fig. 5. Background discrimination on HEGRA CT1 (Kranich 2002). Data from the 1997 Markarian 501 flare. The ALPHA parameter is the angle between the major axis of the image and the line connecting the source location with the center of gravity of the image. ALPHA is small for showers coming from the direction of the source. Cuts in ALPHA and the shape parameters can achieve a background suppression factor of about 200.

sphere can be observed with a variety of detectors on a relatively large area on the ground around the hypothetical impact point of the photon. Gamma rays initiate electromagnetic showers of particles, a multiplicative process started by a e^\pm pair production in the electric field of an atmospheric nucleus. The electrons and positrons give rise to secondary gammas via *bremstrahlung*, which in turn produce more e^\pm pairs. The process goes on until the average energy of the shower particles drops below a critical value (≈ 100 MeV) beyond which the ionization and Compton scattering processes dominate. At this point the shower reaches its maximum development, and then gradually extinguishes. A view of the development of an air shower according to a Monte Carlo simulation is shown on the left panel of Fig. 1.

Throughout the shower development, the electrons and positrons which travel faster than the speed of light in the air emit Cherenkov radiation. Cherenkov photons from a single shower arrive on Earth as a short pulse of a few nanoseconds duration, and spread over a large area, roughly a disk of several hundred meter diameter (see Fig. 2). This constitutes the basis of the most successful technique of ground-based gamma ray astronomy, that of Imaging Atmospheric Cherenkov Telescopes (IACTs). After accounting for atmospheric extinction (due mainly to Rayleigh and Mie scattering), the spectrum of Cherenkov light at ground peaks in the near ultraviolet, around 330 nm. A telescope consisting of a large mirror and a camera of fast photodetectors can obtain a Cherenkov image of the shower above the fluctuations of the light of the night sky. Note that such device will be sensitive to any shower whose Cherenkov light pool contains the telescope, and hence the effective gamma-ray collection area of an IACT is of the order of 10^5 m².

2.1. Background rejection

One of the drawbacks of the IACT technique is the presence of a heavy background: air showers initiated by cosmic ray nuclei are detected by IACTs at a much higher rate

than gammas, even during the observation of the strongest gamma sources. These hadronic showers are wider and more irregular than their electromagnetic counterparts (see right panel of Fig. 1), a fact that can be used in the off-line image analysis to reject most of them, following the methods first proposed by Hillas (1985). The shapes of shower images are parametrized by the momenta, up to second order, of the light distribution on the camera (Fig. 3). An example of how this analysis is performed for the HEGRA CT1 telescope is shown in Fig. 4 and 5, taken from Kranich (2002). Besides, because of the isotropy of the cosmic radiation, the images of hadronic showers have random orientations (cf. Fig. 3, right), whereas the cigar-shaped images of gamma rays from a point-like source are oriented towards the source location on the camera (Fig. 3, left), much like the tracks of shooting stars do in long-exposure pictures of meteor showers. Consequently, when pointing the telescope towards a gamma-ray source, the signal will appear as an excess of shower images aligned with the camera center (see Fig. 5). This orientation parameter (ALPHA) is the only available tool to discriminate the otherwise irreducible background of cosmic ray electrons, which produce electromagnetic showers identical to those started by gamma rays.

From the analysis of the images of showers surviving the background discrimination procedure, the energy spectrum of the observed source can be determined. The energy resolution of an IACT varies between 15 and 30% (statistical error), depending on energy, and is ultimately limited by the systematic error due to the uncertainty in the atmospheric absorption of Cherenkov light. An example of such a spectrum, obtained with the HEGRA stereoscopic system of IACTs (Aharonian et al. 1999) is shown on Fig. 9 (left).

3. The gap in the electromagnetic spectrum

The energy threshold of an IACT is determined by its Cherenkov light collection efficiency, which depends mainly on the mirror size and

reflectivity, and on the photon detection efficiency of the camera. A typical IACT camera consists of an array of photomultipliers of average quantum efficiency in the spectral range of interest between 10 and 20%. The mirror size of Cherenkov telescopes operational during the past fifteen years ranged between 5 and 70 m², resulting in energy thresholds of 300 GeV or higher. On the other hand, space instruments are not sensitive above ≈ 10 GeV, where the photon fluxes are too low for the limited collection areas of satellite-borne detectors (less than 1 m²). The band between 10 and 300 GeV is still unexplored.

A few novel experiments aim at opening this new window for astronomy, both from space, with projects like AGILE (Mereghe et al. 1999) and GLAST (Gehrels et al. 2001) and from ground, with new generation IACTs like CANGAROO III (Mori et al. 2001), HESS (Hofmann et al. 2001), VERITAS (Quinn et al. 2001) and MAGIC (Barrio et al. 1998). The exploration of this energy range is deemed of key importance for the understanding of the processes going on in a number of astrophysical phenomena, like the high energy emission from the jets of AGNs, the mechanisms operating in gamma-ray pulsars, the nature of the still mysterious gamma-ray bursts (GRBs) and the yet unanswered question of the

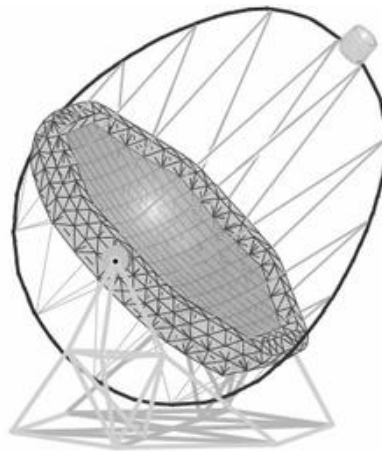


Fig. 6. Sketch of the frame of the MAGIC telescope.

origin of cosmic rays. It is expected that a large number of sources, somewhere in between the 10 firm detections above 300 GeV and the 271 objects in the EGRET catalog, will be observable by MAGIC and other concurrent instruments.

4. The MAGIC telescope

The 17 m diameter f/1 MAGIC telescope is the largest of the new generation IACTs. MAGIC has been built in the Canarian island of La Palma (28.8 N, 17.9 W) at the *Roque de los Muchachos* observatory (ORM), 2200 m above sea level. Its 234 m² parabolic dish is composed of 956 49.5 × 49.5 cm² all-aluminum spherical mirror tiles mounted on a lightweight (< 10 ton) carbon fibre frame (Fig. 6). The parabolic shape was chosen to minimize the time spread of the Cherenkov light flashes on the camera plane, which allows to reduce the rate of fake events induced by night-sky background light. Each mirror is made of an aluminum honeycomb structure, on which a 5 mm plate of AlMgSi1.0 alloy is glued. The aluminum plate of each tile is diamond-milled to achieve the spherical reflecting surface with the radius of curvature most adequate for its position on the paraboloid. A thin quartz layer protects the mirror surface from aging. Mirrors are grouped in panels of three or four, which can be oriented during the telescope operation through an active mirror control system to correct for the possible deformations of the telescope structure.

While all other new generation Cherenkov telescopes aim at the improvement of sensitivity and energy resolution in the 100 GeV regime by using stereoscopic systems of relatively small (10 m) telescopes, MAGIC, through the choice of a single huge reflector, will achieve the lowest energy threshold among IACTs, of about 30 GeV. Its altazimuth mount can point to anywhere in the sky in less than 20 seconds, a unique feature which is essential for the study of transient events like GRBs.

4.1. The camera

The MAGIC camera is equipped with 576 6-dynode compact photomultipliers (PMs), of 20% average quantum efficiency in the 300 - 500 nm range (Ostankov et al. 2000). Each PM is coupled to a small light collecting cone to maximize the active surface of the camera. The total field of view of the camera is about 4°, divided into two sections: an inner hexagon of 396 small pixels, of about 3 cm (0.1°) diameter, and four outer rings of 6 cm diameter PMs (see Fig. 7). The use of larger pixels in the outer zone reduces the cost of the camera, while the quality of the image, already limited in this zone by the coma aberration, is not deteriorated significantly.

4.2. Trigger and readout electronics

The analog signals from the PMs are transformed into light pulses using VCSELs (Vertical Cavity Surface Emitting Lasers), and transported via optical links to the control house, about 100 m away from the telescope. Optical signal transport reduces the need for heavy coaxial cables and guarantees minimal degradation of the pulse shape. A fast 2-level trigger system (Bastieri et al. 2001) starts the data acquisition (DAQ) whenever N neigh-

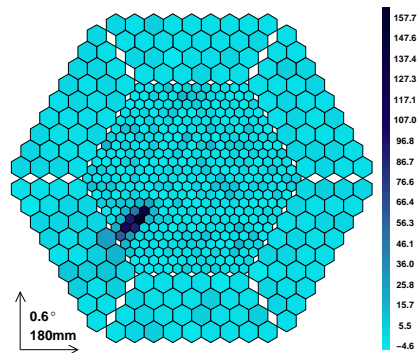


Fig. 7. Schematic drawing of the 576-pixel camera of the MAGIC telescope. A simulated gamma event of energy 50 GeV and impact parameter 90 meter is displayed.

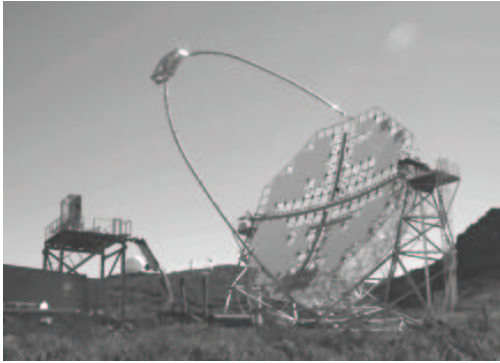


Fig. 8. View of the MAGIC telescope in October 2002, right before the installation of the camera, visible on the access tower on the left. About 40% of the mirrors (covered at the time by protective white foils) were already in place.

bouring pixels fire within a coincidence window Δt of a few nanoseconds. All the trigger parameters will be fine-tuned in the commissioning phase of the telescope. Simulations show that reasonable values could be $N = 4$, $\Delta t = 6$ ns for a pixel threshold of about 8 photoelectrons. A programmable second level trigger, which can sustain rates of up to 1 Mhz, offers the possibility of using fast ($\approx 60 - 80$ ns) pattern recognition routines to perform some background rejection already at trigger level.

The pixel signals are stretched, split into a high- and a low-gain branch (to enlarge the dynamic range), and then digitized using fast (300 MHz), 8-bit Flash ADCs. The maximum event readout rate of the DAQ will be about 1 kHz. As of May 2003, the first tests of the whole DAQ chain and other subsystems are under way at the ORM. About 40% of the mirror surface is already installed (see Fig. 8), the camera and the trigger are fully operational, and the readout of all 576 channels is expected to be working by the Summer. Calibration runs on the Crab Nebula (the standard candle in high energy gamma-ray astronomy) will start in October, and the first observational campaign is due for 2004.

5. The Physics goals of MAGIC

The most relevant Physics questions that will be addressed by MAGIC are the following:

5.1. Active Galactic Nuclei

The observation of nearby blazars at TeV energies with the previous generation of IACTs have been extremely fruitful. The fast flux variations observed from BL Lacs Mkn 421 and Mkn 501 (Gaidos et al. 1996; Aharonian et al. 1999b) indicate that the emission region is very small, less than one light-day (Hillas 1999), and probably very close to the central supermassive black hole. MAGIC will provide better data on these and other similar objects, and will take part in multi-wavelength observation campaigns which will contribute to the understanding of the emission processes occurring in the jets of AGNs. A recent result from the HEGRA collaboration on the giant radiogalaxy M87 (Aharonian et al. 2003) hints at the possibility that blazars are not the only subclass of AGNs capable of emitting GeV-TeV radiation.

5.2. The gamma-ray horizon

Due to the absorption of gamma-rays through interaction with the extragalactic background light (see Fig. 9), only a few nearby blazars have been observed up to now by ground-based gamma telescopes. The low threshold of MAGIC will extend the observable gamma Universe well beyond the limits of the present TeV instruments. Furthermore, if a large sample of AGNs at different redshifts is detected by MAGIC, an indirect measurement of the infrared background density may also be feasible.

5.3. Gamma-ray pulsars

Two different models have been proposed to explain the mechanism of the gamma-ray emission observed by EGRET from six galactic pulsars. The models differ on the location of the emission region: near the magnetic poles (polar cap) or in the outer part of the pul-

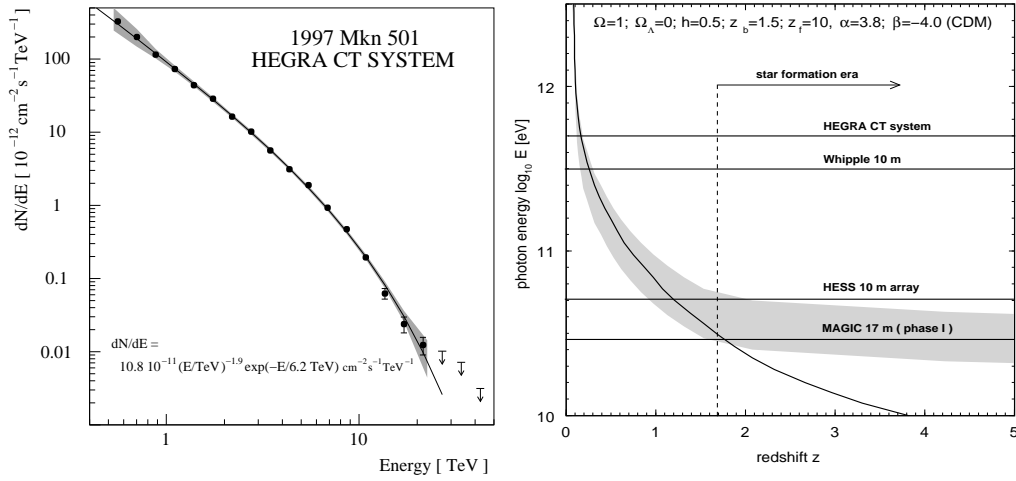


Fig. 9. Left: spectrum of the BL Lac object Markarian 501 ($z = 0.034$) as determined by the HEGRA system of Cherenkov telescopes during its 1997 flare (Aharonian et al. 1999). The spectrum shows a cutoff at a few TeV which is probably a consequence of attenuation of high energy gamma rays through interaction with diffuse extragalactic background radiation ($\gamma\gamma \rightarrow e^+e^-$). Right: gamma-ray horizon, taken from Mannheim (1999). For a given energy, the gamma ray horizon is defined as the distance for which the optical depth τ of the e^\pm pair production process equals 1. The grey band is an estimate of the horizon based on the available upper and lower limits for the flux of the present-day optical to UV diffuse background, while the solid curve results from assuming a star formation rate with an extended plateau. By lowering the energy threshold, new generation Cherenkov telescopes like MAGIC are expected to detect extragalactic sources up to $z = 1.5$ and beyond.

sar magnetosphere (outer gap). The two theories predict slightly different cutoff energies, around a few tens of GeV, but observations in this range have not been possible to date. The detection (or lack of) of a signal from known pulsars with MAGIC will shed some light on this problem. The suggestion that many of the EGRET unidentified sources are actually radio quiet pulsars can also be tested.

5.4. The origin of cosmic rays

More than 90 years after their discovery, the origin of cosmic rays is still unclear. Despite shell-type supernova remnants have long been considered (mainly on grounds of energy budget arguments) the best candidates for the acceleration of the galactic cosmic ray nuclei, the direct proof of this hypothesis is still missing. For long, a signature of gamma rays

from π^0 decay has been searched unsuccessfully in observations of several SNRs: the few positive detections of gamma signals can be well explained as the result of the inverse Compton interactions of high energy electrons with ambient photons. Deep field observations of promising candidates will be a part of the MAGIC observation campaigns.

5.5. Gamma Ray Bursts

Among new generation IACTs, MAGIC is the only one suited for the search for GRBs, due to its low threshold (30 GeV in the first phase), and also to its capability for fast slewing. EGRET has detected 4 photons above 1 GeV from GRBs, and even a 18 GeV photon from GRB940217 (Hurley et al. 1994). Also the MILAGRITO experiment may have detected TeV photons from another burst,

GRB970417a. Extrapolations at MAGIC energies predict that one or two GRBs per year may be detectable by our instrument. A fast alert from satellite instruments (like the SWIFT mission to be launched end of this year) will be anyhow essential in order to allow MAGIC to catch any GRB before the end of the event. Apart from constraining GRB models, the determination of the light curve at GeV energies may be used, for instance, for tests of quantum gravity models, like the predicted Lorentz invariance deformation which would imply a small delay in the arrival of high energy photons.

6. Conclusions

The MAGIC telescope will start operations soon, allowing for the first time to look into the 30 - 300 GeV energy band of the electromagnetic spectrum. A new window for the observation of the Universe is about to be opened.

Acknowledgements. A. Moralejo acknowledges the receipt of a postdoctoral fellowship from the Spanish MECD.

References

- Aharonian, F. A. et al. 2003, A&A 403, L1
- Aharonian, F. A. et al. 1999, A&A 349, 11
- Aharonian, F. A. et al. 1999b, A&A 342, 69
- Barrio, J. A. et al. 1998, MPI Munich report, MPI-PhE/98-5
- Bastieri, D. et al. 2001, NIM A 461, 521
- Gaidos, J. A. et al. 1996, Nature 383, 319
- Gehrels, N. et al. 2001, AIP Conf. Proc. 558, 3
- Hartman, R. C. et al. 1999, ApJS 123, 79
- Hillas, A. M. 1985, Proc. 19th ICRC (La Jolla) 3, 445
- Hillas, A. M. 1999, Astroparticle Physics 11, 27
- Hofmann, W. for the HESS Collaboration 2001, Proc. 27th ICRC (Hamburg), 2785
- Hurley, K. et al. 1994, Nature 372, 652
- Kranich, D. 2002, Ph. D. thesis, Technischen Universität, Munich
- Mannheim, K. 1999, Rev.Mod.Astron. 12, 101
- Meregheiti S. et al. 1999, Proc. GeV-TeV Gamma-Ray Astronomy Workshop, Snowbird, Utah, AIP Proc. Conf. 515, 467
- Mori, M. for the CANGAROO Collaboration 2001, Proc. 27th ICRC (Hamburg), 2831
- Ostankov, A. et al. 2000, NIM A 442, 117.
- Quinn, J. for the VERITAS Collaboration 2001, Proc. 27th ICRC (Hamburg), 2781
- Weekes, T. C. et al. 1989, ApJ 342, 379